Ni activated Mo_2C by regulating the interfacial electronic structure for highly efficient lithium-ion storage

Donglei Guo[a,1], Mengke Yang[a,b,1], Shu Xu[a], Shuping Zhu[a], Guilong Liu[a], Naiteng Wu[a], Ang Cao[c], Hongyu Mi[b,*] and Xianming Liu[a,*]

[a] Key Laboratory of Function-oriented Porous Materials, College of Chemistry and Chemical Engineering, Luoyang Normal University, Luoyang, 471934, P. R. China.

*Email: myclxm@163.com

[b] State Key Laboratory of Chemistry and Utilization of Carbon Based Energy Resources, School of Chemical Engineering and Technology, Xinjiang University, Urumqi, 830046, P. R. China.

*Email: mmihongyu@163.com

[c] Department of Physics, Technical University of Denmark, Lyngby 2800, Denmark.

[1]These authors contributed equally.

Experimental Section

Characterizations: The phase compositions of as-prepared samples were determined by the X-ray diffraction (XRD). The structure and morphologies were characterized by the field-emission scanning electron microscope (FESEM, Sigma 500) and a H-8100 transmission electron microscopy (TEM). The energy dispersive spectrometer (EDS) and element maps were taken on a Sigma 500 FESEM unit. The Raman spectra were collected on an Invia Raman spectrometer with the excitation laser wave-length of 633 nm. The electronic conductivity of the samples was achieved by the resistivity tester (ST2253y). The X-ray photoelectron spectra (XPS) was recorded on an ESCALAB 250 spectrometer (Perkin-Elmer). The specific surface areas were calculated using a standard Brunauer-Emmett-Teller (BET) method on a Belsorp-max surface area detecting instrument.

Electrochemical measurements: The assembly of CR2032 coin cells was carried in an argon-filled glove box with water and oxygen contents below 0.5 ppm. The active materials (80%), conductive carbon black (10%), and polyvinylidene fluoride (PVDF, 10%) were mixed and ground in a mortar. N-Methyl-2-pyrrolidone (NMP) was used as the solvent to make homogeneous slurry. Then, the as-resultant slurry was uniformly pasted on Cu foil current collector and dried in vacuum oven at 80 °C for 12 h and then 120 °C for another 12 h as the working electrode. Lithium metal foil as counter electrode and 1 mol L^{-1} $LiPF_6$ solution with the mixture of EC: DEC: EMC at volume ratio of 1:1:1 as electrolyte. The charge-discharge profiles of the samples were determined by cycling in the potential range of 0.01-3 V at different current rates. Cyclic voltammetry measurements (CV, at different scanning rates) and electrochemical impedance spectroscopy (EIS, in the frequency range from 100,000 to 0.01 Hz) were investigated on a Parstat 4000+ workstation (Princeton Applied Research).

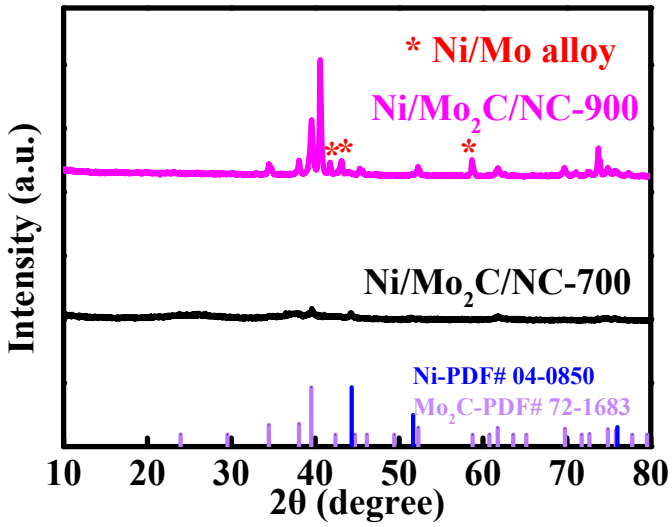

Fig S1. XRD patterns of Ni/Mo_2C/NC-700 and Ni/Mo_2C/NC-900.

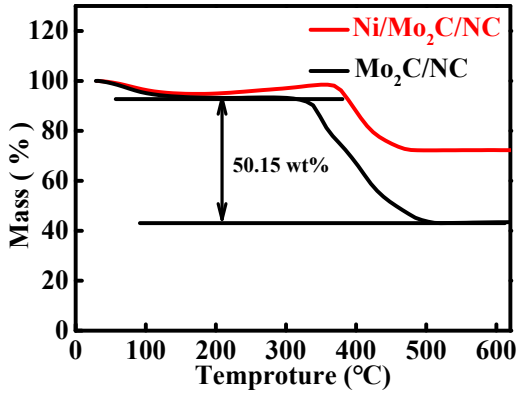

Fig. S2 TGA curves of Ni/Mo_2C/NC and Mo_2C/NC.

The TGA analysis of Ni/Mo_2C/NC and Mo_2C/NC was carried out to calculate the carbon content in Ni/Mo_2C/NC. The Mo_2C/NC and Ni/Mo_2C/NC samples were prepared with the same annealed temperature and precursor, just with or without the Ni. The increasing mass of Ni/Mo_2C/NC is corresponded to the oxidation of Ni and Mo_2C. The carbon content in Ni/Mo_2C/NC is determined to be about 62.69 wt%.

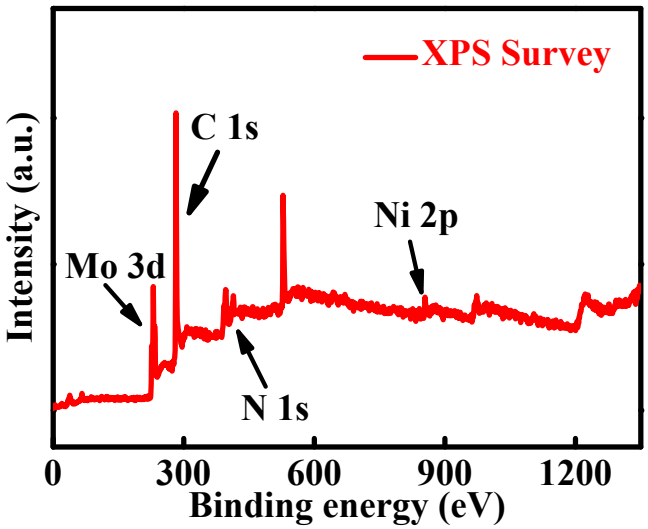

Fig S3 XPS survey spectrum of Ni/Mo_2C/NC.

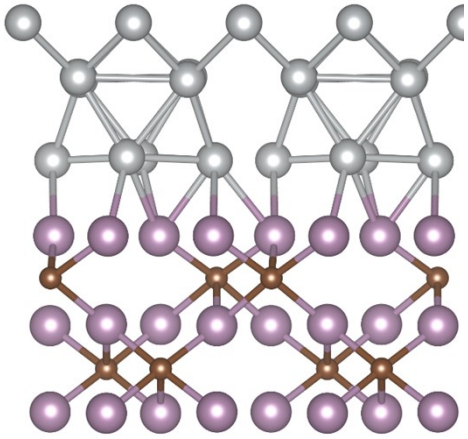

Fig S4 The optimized model of Ni/Mo_2C.

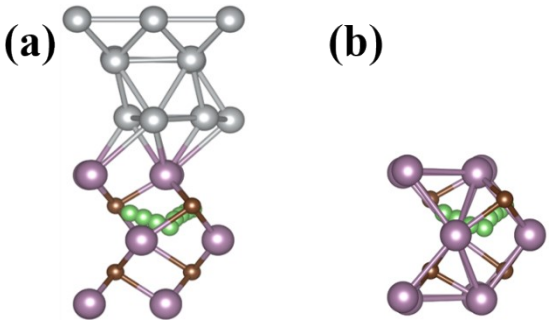

Fig S5 The migration paths of Li^+ in Ni/Mo_2C (a) and Mo_2C (b).

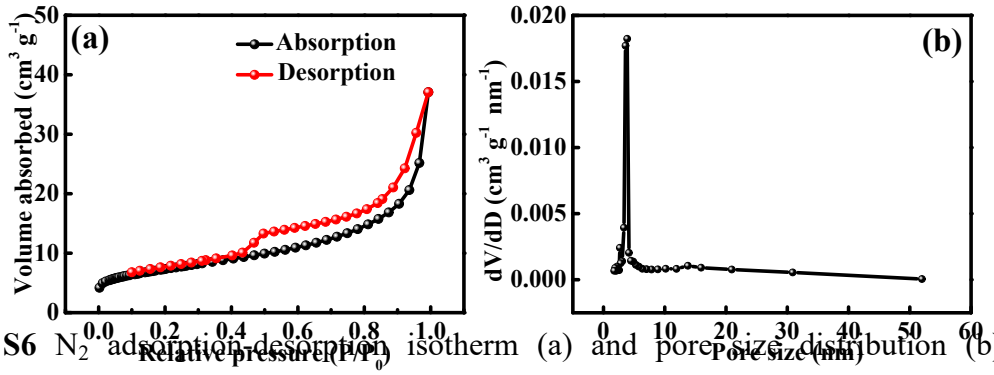

Fig S6 N_2 adsorption-desorption isotherm (a) and pore size distribution (b) of Ni/Mo_2C/NC according to the NLDFT model.

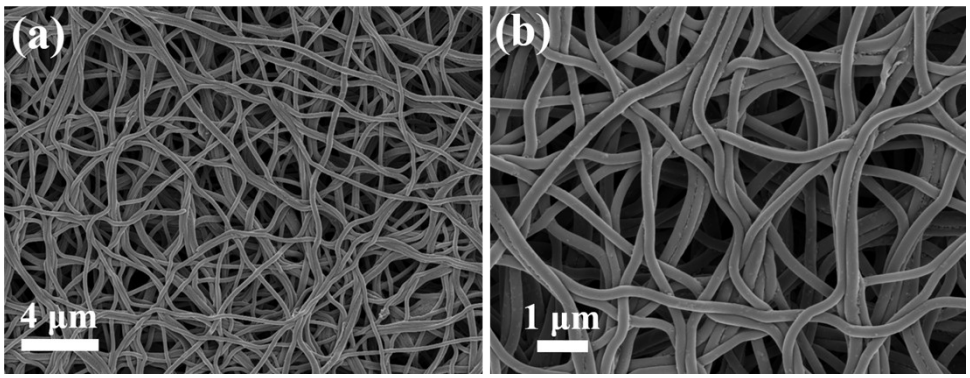

Fig. S7 FESEM images of Ni-Mo-PAN precursor.

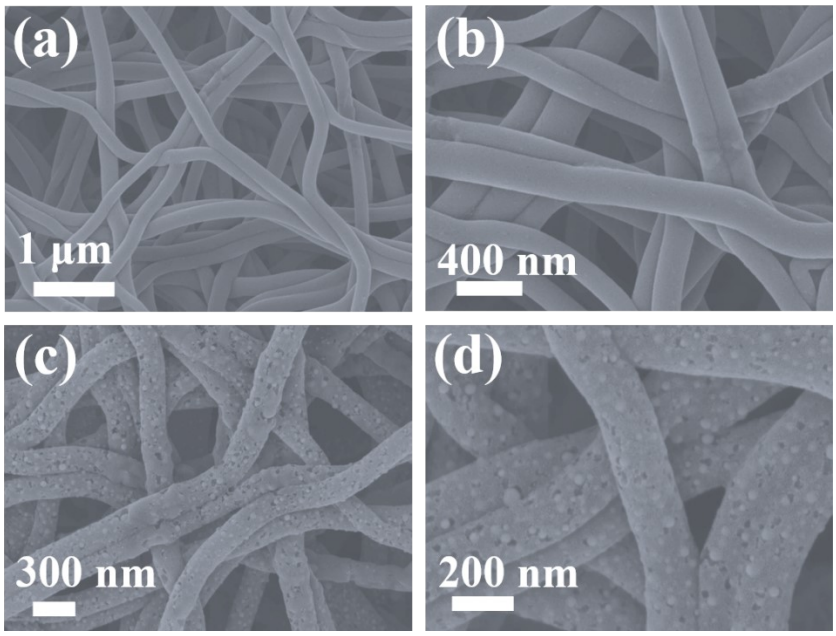

Fig S8 (a, b) FESEM images of Ni/Mo_2C/NC-700. (c, d) FESEM images of Ni/Mo_2C/NC-900.

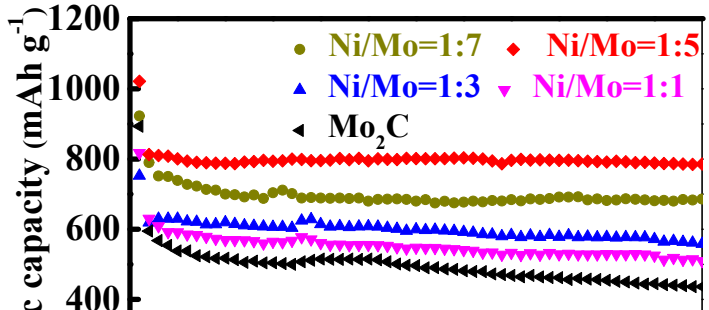

Fig S9 Comparison of the cyclic performances of Ni/Mo_2C/NC with different contents of Ni.

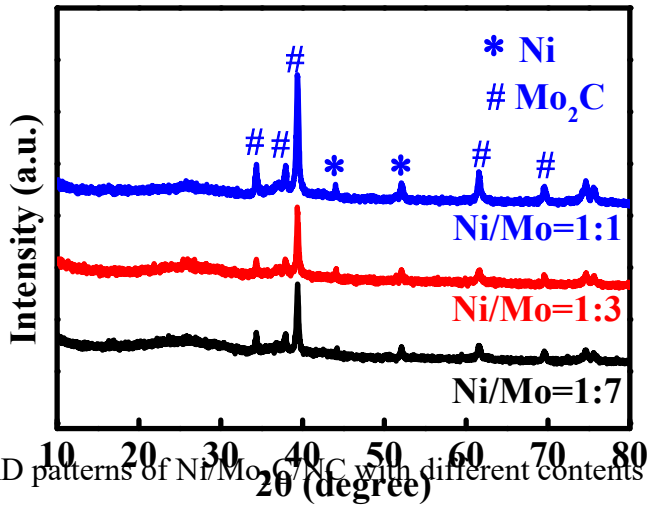

Fig S10 XRD patterns of Ni/Mo_2C/NC with different contents of Ni.

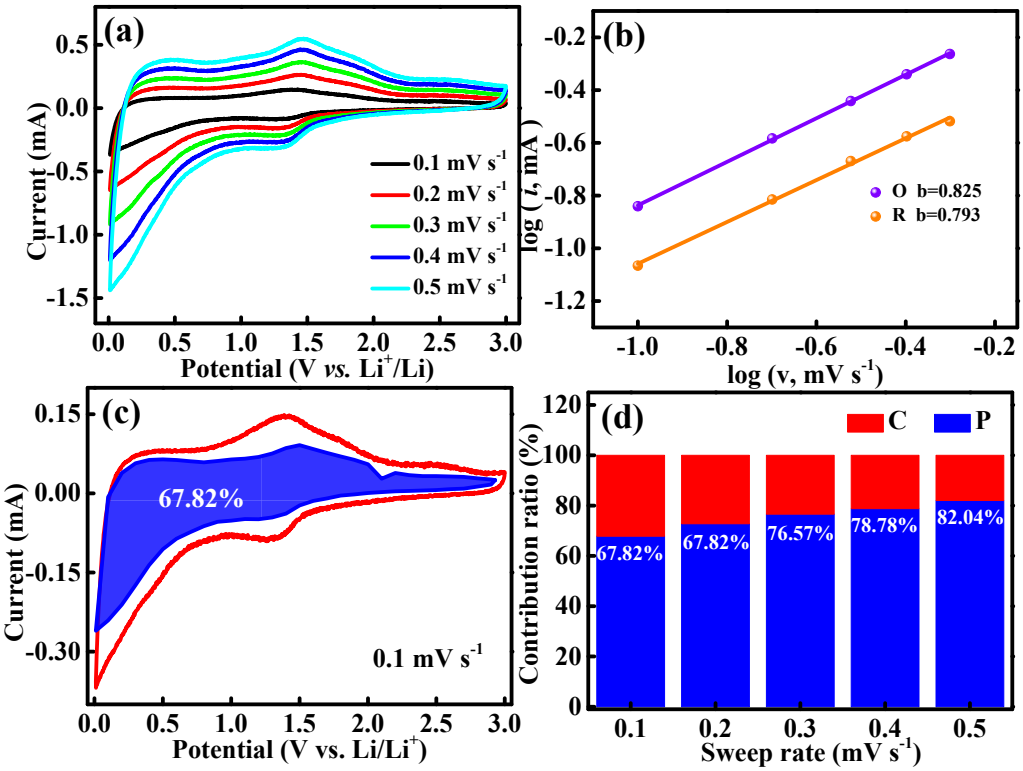

Fig S11 (a) CV curves of Mo_2C/NC at different scan rates. (b) Log (i) vs. log (v) plots at each redox peak of Mo_2C/NC. (c) Capacitive contribution to charge storage of Mo_2C/NC at a scan rate of 0.1 mV s^{-1}. (d) Percentage of capacitance contribution of Mo_2C/NC at different scan rates.

Table S1. Comparison of the electrochemical performance of Ni/Mo_2C/NC with reported Mo_2C-based anodes for LIBs.

Mo_2C-based materials	Rate capability	Cyclic performance	Ref.
	Current density (A g^{-1})/Capacity (mA h g^{-1})	Current density (A g^{-1})/Cycle number/Capacity (mA h g^{-1})	
3DHP-Mo_2C	3/255.6	1/600/481.4	[r1]
Mo_2C/C	3/648.1	0.75/650/899	[r2]
Mo_2C/C/rGO	4/200	0.5/1600/630	[r3]
Mo_2C/C NRs	6/100	1/1000/300	[r4]
Mo_2C@CNT	16/225	1.6/750/878	[r5]
Mo_2C-C	2/335.4	2/50/308	[r6]
Mo_2C/N-C MHNWs	5/486.3	2/700/732.9	[r7]
Mo_2C@C-GA	5/669.3	1/200/804.5	[r8]
C@α-Mo_2C	20/204	5/2000/400	[r9]
Mo_2C(52.6%)/GR	1.6/310	0.1/100/813	[r10]
HP-Mo_2C-C	10/317	0.3/100/873.6	[r11]
This work	10/344.1	2/1800/412.7	

References

[r1] T. Meng, L. R. Zheng, J. W. Qin, D. Zhao and M. H. Cao, *J. Mater. Chem. A*, 2017, **5**, 20228-20238.

[r2] F. C. Lyu, S. S. Zeng, Z. F. Sun, N. Qin, L. J. Cao, Z. Y. Wang, Z. Jia, S. F. Wu, F. X. Ma, M. C. Li, W. X. Wang, Y. Y. Li, J. Lu and Z. G. Lu, *Small*, 2019, **15**, 1805022.

[r3] K. K. Halankar, B. P. Mandal, S. Nigam, C. Majumder, A. P. Srivastava, R. Agarwal and A. K. Tyagi, *Energy Fuels*, 2021, **35**, 12556-12568.

[r4] Z. W. Yang, H. F. Wang, B. S. Cheng, C. Yue, G. Z. Liu, R. T. Zheng, F. Hu and J. Shu, *Energy Technology*, 2020, **8**, 2000189.

[r5] B. Yu, D. X. Yang, Y. Hu, J. R. He, Y. F. Chen and W. D. He, *Small Methods*, 2018, **3**, 1800287.

[r6] Q. Gao, X. Y. Zhao, Y. Xiao, D. Zhao and M. H. Cao, *Nanoscale*, 2014, **6**, 6151-6157.

[r7] L. C. Yang, X. Li, S. N. He, G. H. Du, X. Yu, J. W. Liu, Q. S. Gao, R. Z. Hu and M. Zhu, *J. Mater. Chem. A*, 2016, **4**, 10842-10849.

[r8] H. L. Xin, Y. Hai, D. Z. Li, Z. Z. Qiu, Y. M. Lin, B. Yang, H. S. Fan and C. Z. Zhu, *Appl. Surf. Sci.*, 2018, **441**, 69-76.

[r9] F. Hu, Z. M. Liu, C. Yue, J. Xiang and T. Song, *ChemistrySelect*, 2018, **3**, 8395-8401.

[r10] B. B. Wang, G. Wang and H. Wang, *J. Mater. Chem. A*, 2015, **3**, 17403-17411.

[r11] Y. Xiao, L. R. Zheng and M. H. Cao, Nano Energy, 2015, 12, 152-160.